Chloroform Anion Fragmentation in Liquid Methylcyclohexane: $t^{-0.6}$ Simulation of the Geminate Ion Kinetics

Rolf E. Bühler,*,† Anastasia S. Domazou, and Yosuke Katsumura‡

Laboratory for Physical Chemistry, ETH Zürich, Switzerland

Received: December 16, 1998

The chloroform anion in liquid methylcyclohexane (MCH) fragments during the time scale of geminate ion recombination (143 K ≤ T ≤ 193 K). Its lifetime can only be determined if the geminate ion kinetics can be calculated. The $t^{-0.6}$ semiempirical law is used. Because $CHCl_3$ quenches M^{+}*, the precursor of the solvent radical cation MCH^+, much less effectively than N_2O, the fragmentation of M^{+}* to produce the methylcyclohexene cation ($MCHene^+$) has to be considered by theory. The $t^{-0.6}$ simulation therefore was modified to include the two parallel reactions of the M^{+}* decay, which are forming mixed ion pairs ($MCHene^+$, MCH^+/X^-). It is found that mixed pairs are still describable by the $t^{-0.6}$ linearity, yet the mobility factor δ (slope of $t^{-0.6}$) is now λ-dependent. Complete simulation of the ionic mechanism yields the following results: (1) The fragmentation rate constant for $CHCl_3^-$ is $k_1(143\ \mathrm{K}) = (3.6 \pm 0.3) \times 10^6\ \mathrm{s}^{-1}$ with $E_{act} = 4.6 \pm 0.5$ kJ/mol and log$A = 8.2 \pm 0.2$. The lifetime of 280 ns is substantially larger than expected from gas phase data. (2) By applying the known G_{fi} values to the free ion spectra at 143 K, 153 K, and 173 K, the absorption coefficients of the $CHCl_3^-$ band were determined and a Lorentzian line shape fitted: $\lambda_{max} = 470$ nm, $\epsilon_{max} = 1900 \pm 30\ \mathrm{M}^{-1}\ \mathrm{s}^{-1}$ and a width of hwhm $= 28 \pm 2$ nm. (3) Assuming that the M^{+}* fragmentation (k_{frag}) and the natural relaxation to MCH^+ (k_0) are the same as in N_2O-saturated MCH, the quenching rate constant at 143 K may be derived: $k_2(M^{+}* + CHCl_3 \rightarrow MCH^+) = (7.7 \pm 2.6) \times 10^6\ \mathrm{M}^{-1}\ \mathrm{s}^{-1}$. Quenching by $CHCl_3$ therefore is about four times slower than by N_2O; the yield of the olefinic cation ($MCHene^+$) is strongly increased relative to the MCH^+ yield. Furthermore, the ratio quenching/fragmentation with chloroform as solute is found to increase with temperature, suggesting that fragmentation at room temperature might have much less importance.

I. Introduction

From pulse radiolysis experiments with a methylcyclohexane (MCH) solution of chloroform $CHCl_3$ at 143 K we assigned several years ago a transient absorption band at 470 nm to the anion of chloroform, $CHCl_3^-$,[1] (see Figure 1a). Its decay at late times was compatible with geminate ion kinetics, as tested by the semiempirical $t^{-0.6}$ kinetic law[2] (see below). However, at early times deviations from the $t^{-0.6}$ linearity indicated that other ionic processes, such as ion fragmentations, must interfere with neat geminate ion kinetics.[3]

In the meanwhile we have published details of the $t^{-0.6}$ kinetic law, particularily to include overlapping ionic reactions,[3−5] and we were able to identify the solvent radical cation MCH^+ and its reaction with positive scavengers (e.g., norbornadiene).[4] We also detected the existence of a precursor to MCH^+, called M^{+}*, some excited state of MCH^+.[5] With this knowledge of the ionic mechanism in the solvent MCH it is now possible to understand the details of the anion fragmentation occuring in MCH with chloroform as electron scavenger. The results are given in this paper.

The original $t^{-0.6}$ kinetic law[2] describes the probability of survival of the geminately recombining ions relative to the free ion yield:

$$\frac{G(t)}{G_{fi}} = 1 + \underbrace{0.6\left[\frac{r_c^2}{D}\right]^{0.6}}_{\alpha} t^{-0.6} = \frac{\text{absorbance } (t)}{\text{absorbance } (\infty)} = \frac{A(t)}{\mathrm{IA}} \qquad (1)$$

The absorption may have contributions from both types of ions (sum of both absorption coefficients). Any plot of the absorbance $A(t)$ against $t^{-0.6}$ should be linear. Its intercept IA for $t = \infty$ ($t^{-0.6} = 0$) corresponds to the absorbance of the free ion yield. The slope divided by the intercept IA is called α (or β, γ, etc.). From this value, with the known Onsager radius r_c, an experimental diffusion constant can be derived: $D_{exp} = D^+ + D^-$. Theoretical support for the $t^{-0.6}$ rate law was recently given by Barczak and Hummel.[6] From the many semiempirical theories to simulate the nonhomogeneous, geminate ion kinetics, only the $t^{-0.6}$ rate law is able to explain the experimental results in methylcyclohexane.[3,4]

If geminate ions undergo a reaction, there is a changeover from a primary to a secondary pair of geminate ions, with a first order or pseudo first order rate constant k_1.[4,5] The primary geminate ion kinetics is given by

$$\frac{A_{prim}(t)}{\mathrm{IA}} = [1 + \alpha t^{-0.6}]e^{-k_1 t} \qquad (2)$$

with $\alpha = 0.6\left[\frac{r_c^2}{D_{prim}}\right]^{0.6}$ and $\mathrm{IA} = A_{prim}(\infty)$

† Mailing address: Physical Chemistry, ETH Zürich, Mühlebachstrasse 96, 8008 Zürich, Switzerland.

‡ Permanent address: Nuclear Engineering Research Laboratory, School of Engineering, University of Tokyo, Japan.

10.1021/jp984760w CCC: $18.00
Published on Web 06/11/1999

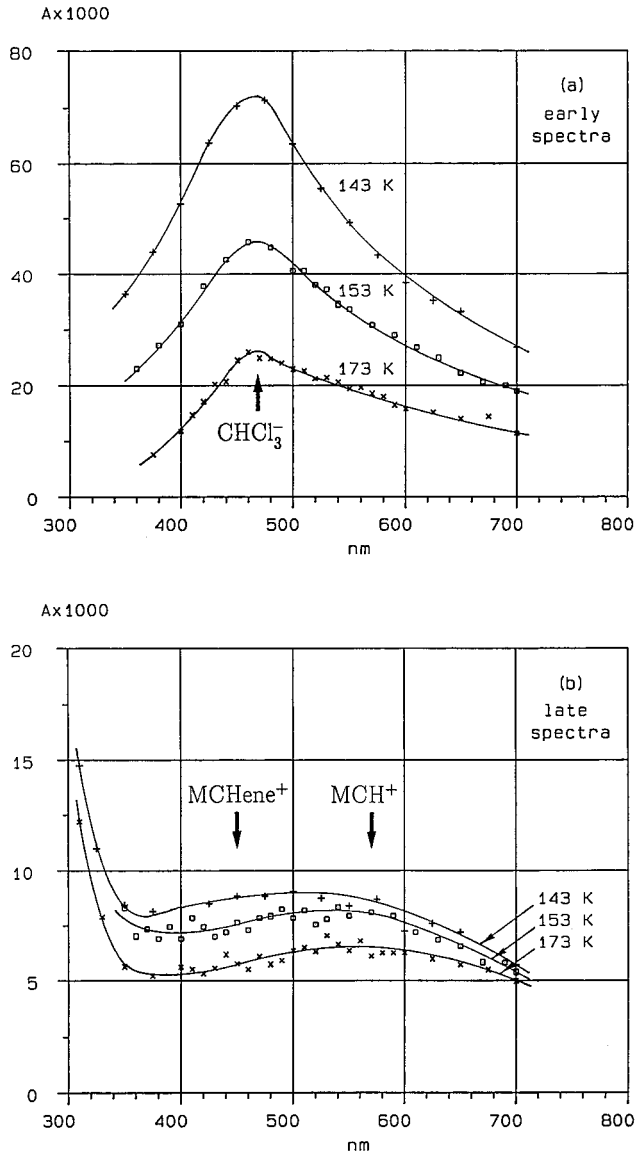

Figure 1. Transient spectra in a solution of $CHCl_3$ in MCH at 143 K (0.3 M), 153 K (0.2 M), and 173 K (0.2 M); (a) early spectra at 200 ns after pulse start; (b) late spectra for 143 K at 20 μs, 153 K at 10 μs, and 173 K at 5 μs after pulse. Absorbance A normalized to 100 Gy.

The secondary geminate ion kinetics is approximated by

$$\frac{A_{sec}(t)}{IB} = [1 + \beta t^{-0.6}]\,[1 - e^{-k_1 t}] \qquad (3)$$

$$\text{with} \qquad \beta = 0.6\left[\frac{r_c^2}{D_{sec}}\right]^{0.6} \qquad \text{and} \qquad IB = A_{sec}(\infty)$$

The sum of primary and secondary ion absorbances then simulates the experimental time profile

$$A(t) = A_{prim}(t) + A_{sec}(t) \qquad (4)$$

The application of this $t^{-0.6}$ simulation to systems, where geminate ion recombination kinetics is complicated by simultaneous ionic reactions, was critically discussed in recent papers by Bühler.[7,8] Because of its simplicity, it is a very powerful tool to study geminate ion mechanisms.

In the previous paper on the precursor M^{+*} [5], it was shown that M^{+*} not only relaxes or quenches to MCH^+ but also fragments to a cation of methylcyclohexene ($MCHene^+$) to some extent. Such parallel ionic reactions do yield mixed pairs of secondary ions: ($MCHene^+$/$Anion^-$) and (MCH^+/$Anion^-$), in this case with quite different mobilities. The consequences on the kinetics so far have not yet been seen in experiments with neat or N_2O-saturated MCH.[5] In the present paper with chloroform as an electron scavenger (and also as quencher of M^{+*}), the $t^{-0.6}$ kinetic theory clearly had to be extended to include such mixed pairs of geminate ions.

II. Experimental

The technique of pulse radiolysis with a Febetron 705 accelerator (Physics International) for 30 ns pulses of 2 MeV electrons has been used as reported.[4,5] Experiments with methylcyclohexane as solvent were performed in the temperature range from 143 to 193 K in the liquid state. The stainless steel cell had an optical path length of 2 cm. A typical dose was between 50 and 150 Gy. Dosimetry was done by calorimetry. The data treatment, kinetic analysis, and data simulation were performed on a PDP 11/73 computer.

All of the experimental signals were corrected for the cell window signal (quartz defects) as described in the previous paper.[4] The origin of shock waves in pulse radiolysis cells and the method to minimize the effect have also previously been discussed in detail.[4,9] As the shock waves are correlated with the speed of sound and are reflected back and forth in the cell, the shock pattern can be identified as periodic signal during earlier times but gets smeared out later on.

Chemicals. Methylcyclohexane (Fluka purum, >98% GC) was passed through a column of aluminum oxide, dried over molecular sieve A4, and then fractionated through a Fischer "Spaltrohrkolonne" with about 30 theoretical plates. Chloroform (Fluka puriss) was used as received.

III. Results

Pulse Radiolysis. Pulse radiolysis of a solution of $CHCl_3$ in MCH, studied at 143, 153, and 173 K, revealed the known spectrum of the $CHCl_3^-$ anion (λ_{max} = 470 nm), as previously assigned at 143 K (Figure 1a).[1] About 10 μs later the characteristic anion band has disappeared (Figure 1b). The weak remaining absorption tends to indicate a wide absorption band peaking between 500 and 600 nm, clearly seen for the spectra at 173 K and 153 K. The late spectrum at 143 K is comparable in shape to the late transient spectrum in a N_2O-saturated MCH.[4] Obviously the $CHCl_3^-$ anion disappears before the geminate ion recombination has completed.

Initial Proposal. The initial proposal for the reaction mechanism is shown in Scheme 1, neglecting any fragmentation of M^{+*}.

SCHEME 1

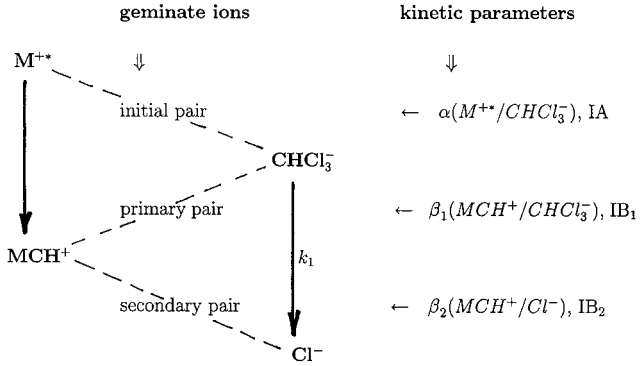

As both anions are of diffusional mobility, the overall mobility must be governed by the high mobility of the radical cation

TABLE 1: Results from the $t^{-0.6}$ Kinetic Simulation

	MCH/N_2O sat.[4]		$MCH/CHCl_3$					
temp K	$\beta_1=\beta_2$[a] $\mu s^{0.6}$	$D_{exp}/10^{-6}$ $cm^2\ s^{-1}$	$[CHCl_3]$ M	δ_{mix} (470 nm)[b] $\mu s^{0.6}$	$\beta(MCH^+/X^-)$[c] $\mu s^{0.6}$	$\gamma(MCHexene^+/X^-)$[c] $\mu s^{0.6}$	$k_1/10^6$ [d] s^{-1}	$k_{tot}/10^6$ [e] s^{-1}
143	3.05	1.73	0.3	9.7	3.0	15.7	3.6 ± 0.3	5.1 ± 0.4
153	2.05	3.05	0.2	4.0	2.0	6.2	4.6 ± 0.4	6.0 ± 0.5
163	1.50	4.52	0.2	2.3	*f*	*f*	5.8 ± 0.5	*f*
173	1.14	6.45	0.2	1.6	0.64	2.8	7.0 ± 0.8	*f*
183	0.88	9.05	0.2	1.15	*f*	*f*	8.0 ± 1.0	*f*
193	0.69	12.3	0.2	0.7	*f*	*f*	~ 10.0	*f*

[a] Called α in ref 4. [b] $\delta_{mix} = \delta_1 = \delta_{2,exp}$. [c] Derived from simulation of $\delta_{mix}(\lambda)$ by using k_Q/k_{frag} from Table 2 and ϵ_i from Figure 8. [d] k_1 for the anion fragmentation $CHCl_3^- \rightarrow Cl^-$. [e] k_{tot} for the M^{+*} decay ($= k_Q + k_{frag}$). [f] Too fast for detection or not measured.

MCH^+ [4] and its precursor M^{+*},[5] as previously determined from N_2O-saturated MCH: $\beta_1 = \beta_2$ as reproduced in Table 1 (from ref 4). Simulations with these data, however, were rather unsatisfactory. The range of $t^{-0.6}$ linearity was very small, implying a long lifetime of $CHCl_3^-$, longer than expected from spectral judgement (Figure 1). The free ion intercept spectra, IB_1 and IB_2, strongly increased with lower temperature, which is against expectation (the free ion yield decreases with temperature[4]). The free ion intercept spectrum IB_2 still showed a strong contribution from the $CHCl_3^-$ band. This contradicts the expected reaction scheme.

Second Proposal. It was realized that a much wider $t^{-0.6}$ linearity range could be achieved if the mobility values $\beta_1 = \beta_2$ were allowed to be free parameters. They turned out to be two to three times larger, corresponding to lower mobilities of the ions. The free ion spectra became comparable with the one found in N_2O-saturated MCH.[4,5] This is also true for the expected temperature dependence. The higher values for $\beta_1 = \beta_2$ could possibly be explained by increased viscosity of the concentrated solution of $CHCl_3$ near or below the melting point (some systems represented supercooled liquids). Yet the nearly constant $\beta_1 = \beta_2$ values in the λ range of the $CHCl_3^-$ band (450 to 550 nm) did not yield satisfactory fits for the rest of the spectrum, particularly for $\lambda \geq 550$ nm. A careful fitting by linear regression revealed the necessity of a λ dependence of the $\beta_1 = \beta_2$ values. These mobility values will now be called $\delta(\lambda)$.

Conclusions. As mentioned in the previous paper,[5] such λ dependences may be expected in systems with mixed pairs of geminate ions, i.e., pairs in which one partner ion is made up of two product ions (from two parallel reactions), possibly with different mobilities. This is the case for all MCH solutions as shown in Scheme 2.[5] The relative yield from the two parallel

SCHEME 2

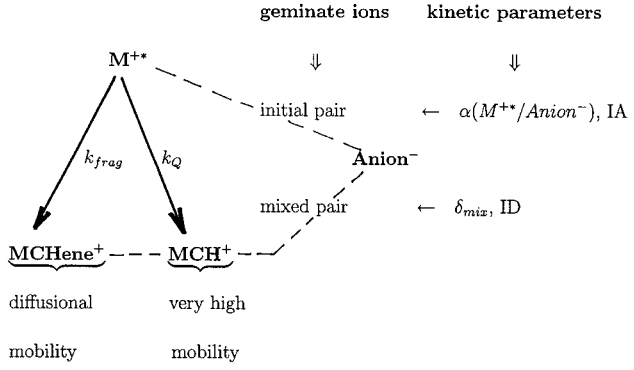

reactions is related to the quenching efficiency of the solute. For the chloroform solutions the ratio of $MCHene^+/MCH^+$ is close to one (see later), making the effect of the λ dependence larger.

In order to understand the geminate kinetics with mixed pairs of geminate ions, the $t^{-0.6}$ simulation theory has to be modified. Theory has to tell whether there is still a linearity with $t^{-0.6}$ for mixed pairs and whether the λ dependent mobility values $\delta(\lambda)$ can be explained.

IV. Theory for Mixed Pairs of Geminate Ions

If one of the initial geminate ions (e.g., the cation A^+) suffers two parallel processes, such as a fragmentation with k_1'' to yield C^+ and simultaneous quenching (or relaxation) with k_1' to yield B^+, then the decay of the initial ion (A^+) produces simultaneously two types of secondary cations (B^+ and C^+), possibly with different mobilities. The decay rate of A^+ is $k_{tot} = k_1' + k_1''$ as shown in Scheme 3.

SCHEME 3

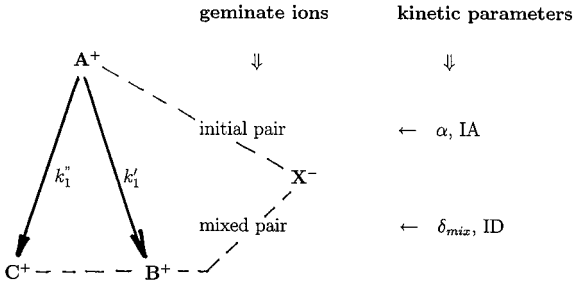

The question arises whether the mixed pairs are still following the $t^{-0.6}$ kinetics, particularly if the mobilities of the two product ions (D_{B^+} and D_{C^+}) should differ. The mobility values of the individual pairs are

$$\beta(B^+/X^-) = 0.6\left(\frac{r_c^2}{D_{B^+/X^-}}\right)^{0.6}$$

$$\gamma(C^+/X^-) = 0.6\left(\frac{r_c^2}{D_{C^+/X^-}}\right)^{0.6} \quad (5)$$

It appears reasonable to assume that each of the secondary pairs follows its own geminate kinetics with β or γ. The overall geminate kinetics is then split into parts, with contributions of k_1'/k_{tot} and k_1''/k_{tot}:

$$G_{sec}(B^+/X^-) = G_{fi}\frac{k_1'}{k_{tot}}(1+\beta t^{-0.6}) = \frac{A_{sec,B}(t)}{(\epsilon_{B^+}+\epsilon^-)lf} \quad (6)$$

$$G_{sec}(C^+/X^-) = G_{fi}\frac{k_1''}{k_{tot}}(1+\gamma t^{-0.6}) = \frac{A_{sec,C}(t)}{(\epsilon_{C^+}+\epsilon^-)lf} \quad (7)$$

where f = conc (M)/G value (1/100 eV) = density (g cm^{-3}) × dose (Gy) × 10^{-7} and l = optical cell length (cm).

On this base, the total absorption A_{tot} due to the secondary ions (B^+, C^+, and X^-) corresponds to

$$A_{tot} = A_{sec,B} + A_{sec,C} \tag{8}$$

Equations 6, 7, and 8 can be rewritten to yield the total absorbance as a function of $t^{-0.6}$

$$A_{tot} = ID[1 + \delta t^{-0.6}] \tag{9}$$

$$\delta = b\beta + (1-b)\gamma \qquad b = \left[1 + \frac{k_1''}{k_1'}\frac{(\epsilon_{C^+} + \epsilon^-)}{(\epsilon_B^+ + \epsilon^-)}\right]^{-1} \tag{10}$$

and an intercept of

$$ID = G_{fi} I f \left[\epsilon^- + \frac{k_1'}{k_{tot}}\epsilon_{B^+} + \frac{k_1''}{k_{tot}}\epsilon_{C^+}\right] \tag{11}$$

This means that the mixed pair of geminate ions still follows the $t^{-0.6}$ kinetics. However, the mobility value δ is λ dependent because of the individual spectral contributions based on the absorption coefficients ϵ_{B^+}, ϵ_{C^+}, and ϵ^- and as long as the two secondary pairs are not of the same mobility ($\beta \neq \gamma$). The intercept ID still corresponds to the free ion yield, yet the positive ion contribution is split into contributions from B^+ and C^+, dependent on the yield ratio k_1'/k''. The application of the eqs 9−11 to the experimental results from chloroform in MCH in this paper is a clear support for this theory.

V. Discussion

The Mechanism. Ionization in a methylcyclohexane solution of chloroform produces a solvent radical cation (in some excited state) and a solvated electron. The latter is captured by $CHCl_3$ faster than our time resolution. There is neither a $CHCl_3^-$ buildup, nor a vanishing e^-_{solv} spectrum detectable for $t \geq 30$ ns. The initial pair of geminate ions therefore is ($M^{+*}/CHCl_3^-$). As M^{+*} undergoes two parallel reactions (fragmentation and quenching) it is followed by two consecutive mixed pairs, the primary with $CHCl_3^-$ and the secondary with Cl^-, due to the anion fragmentation (Scheme 4).

SCHEME 4

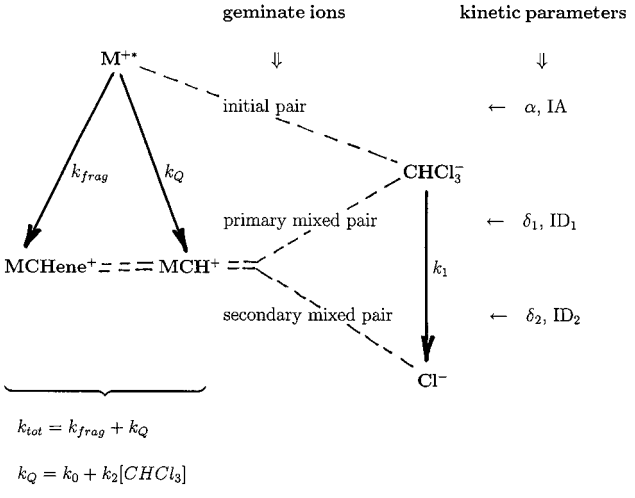

The rate of M^{+*} decay is $k_{tot} = k_{frag} + k_Q$, the sum of fragmentation and quenching by the solute $CHCl_3$ (k_2) and quenching by the solvent or relaxation (k_0).

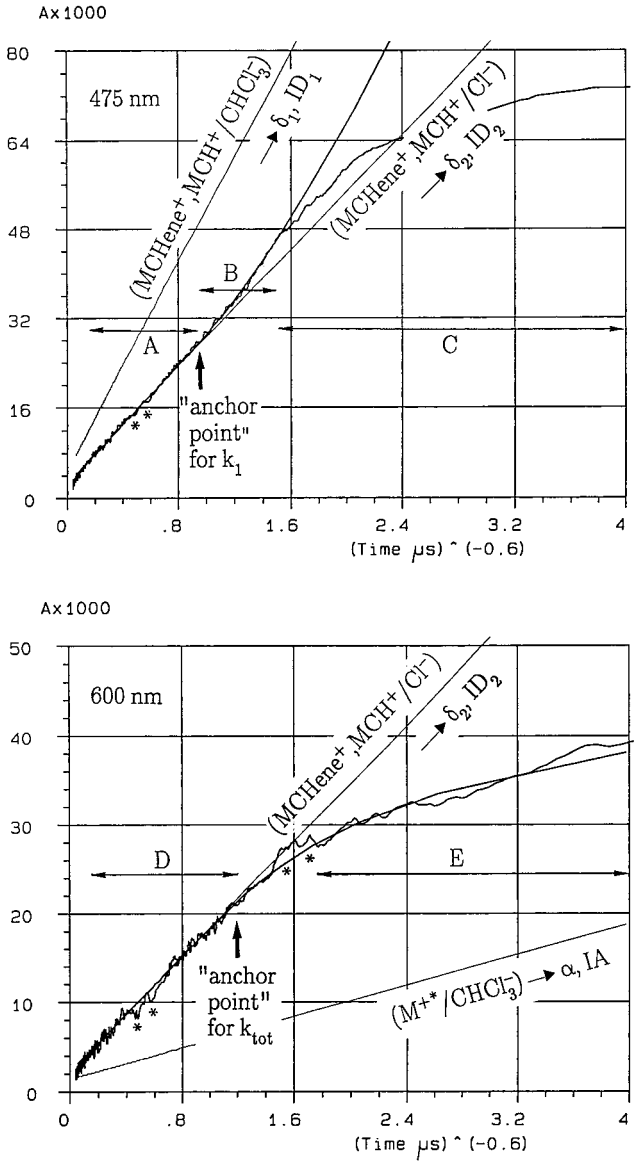

Figure 2. The $t^{-0.6}$ plot of the rate curves in 0.3 M $CHCl_3$ in MCH at 143 K. Simulation corresponds to Scheme 4. The asterisk (*) marks systematic disturbances from shock waves (intensity λ dependent). *A* = absorbance normalized at 100 Gy. (a) 475 nm: simulation of the anion decay k_1 and the linearities for the two mixed pairs of ions. δ_2 and ID_2 from the linearity in range *A*; k_1 from the "anchor point"[10] at $t^{-0.6} \approx 0.95\ \mu s^{-0.6}$; $\delta_1 = \delta_{2,exp}$ (see text); finally ID_1 from curve fitting in the range B. For the downward deviation in range C see Figure 2b. (b) 600 nm (no $CHCl_3^-$ absorption): simulation of the parallel decay of M^{+*} with k_{tot}. δ_2 and ID_2 from the linearity in range D; $k_{tot} = k_Q + k_{frag}$ from the anchor point[10] at $t^{-0.6} \approx 1.2\ \mu s^{-0.6}$; α ($M^{+*}/CHCl_3^-$) = $\beta(MCH^+/CHCl_3^-)$ (see text); and IA from curve fitting in range E.

The $t^{-0.6}$ Plot. See the example in Figure 2 for 143 K. The linearity with $t^{-0.6}$ at low $t^{-0.6}$ values (late times) represents the geminate ion recombination of the secondary mixed pair ($MCHene^+$, MCH^+/Cl^-). At $t^{-0.6} < 0.15\ \mu s^{-0.6}$ (143 K), the free ion recombination is responsible for deviations from linearity (not considered by the $t^{-0.6}$ kinetic theory) and for $t^{-0.6} \gtrsim 0.95\ \mu s^{-0.6}$ the anion fragmentation, $CHCl_3^- \rightarrow Cl^-$, is responsible for the upward deviation from linearity (Figure 2a): The point at $t^{-0.6} \approx 1.0\ \mu s^{-0.6}$ represents the "anchor point"[8,10] and defines the "end" of the anion fragmentation. It allows to determine the rate constant $k_1(CHCl_3^- \rightarrow Cl^-)$ from experiments within the λ range of the $CHCl_3^-$ absorption band, typically between 420 and 530 nm (compare with Figure 7). For $\lambda > 550$

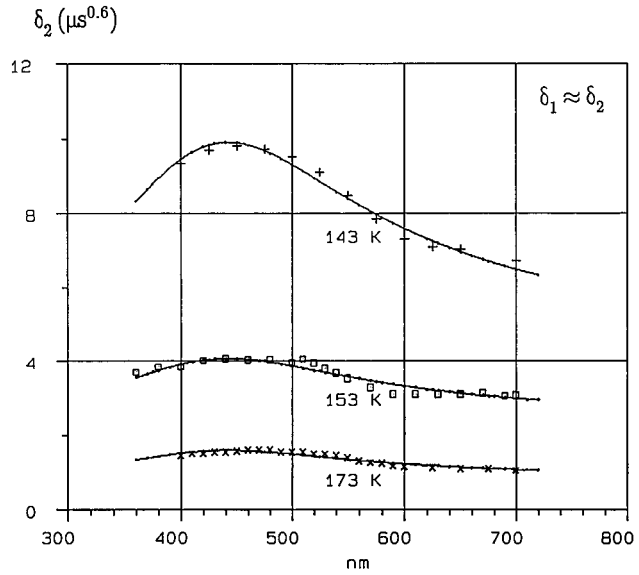

Figure 3. The λ dependence of the mobility value $\delta_2(\lambda)$ for the mixed pair of ions ($MCHene^+$, MCH^+/Cl^-) as measured in MCH solutions of $CHCl_3$ at 143, 153, and 173 K. The theoretical curves are based on eqs 9−11. $\beta(MCH^+/Cl^-)$ and $\gamma(MCHene^+/Cl^-)$ are fitting parameters. Their optimized values are given in Table 1. $\delta_1(MCHene^+, MCH^+/CHCl_3^-) \approx \delta_2$ (see text).

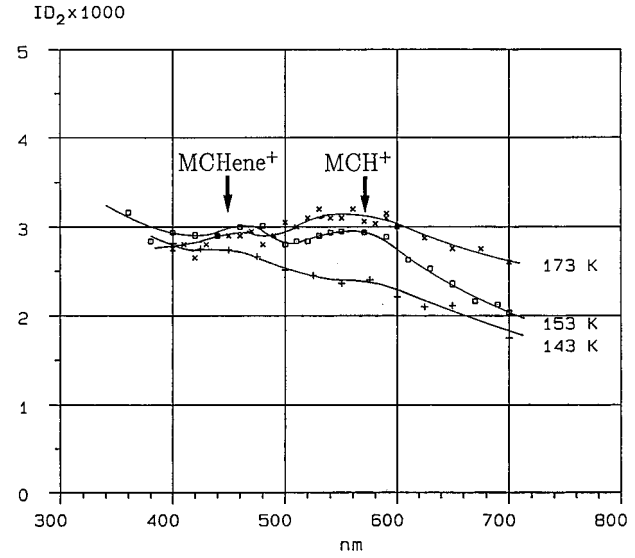

Figure 4. The free ion intercept spectra ID_2 at 143, 153, and 173 K for the secondary mixed pairs of ions ($MCHene^+$, MCH^+/Cl^-). See Scheme 4. There are contributions from $MCHene^+$ (λ_{max} = 450 nm) and MCH^+ (λ_{max} = 570 nm).

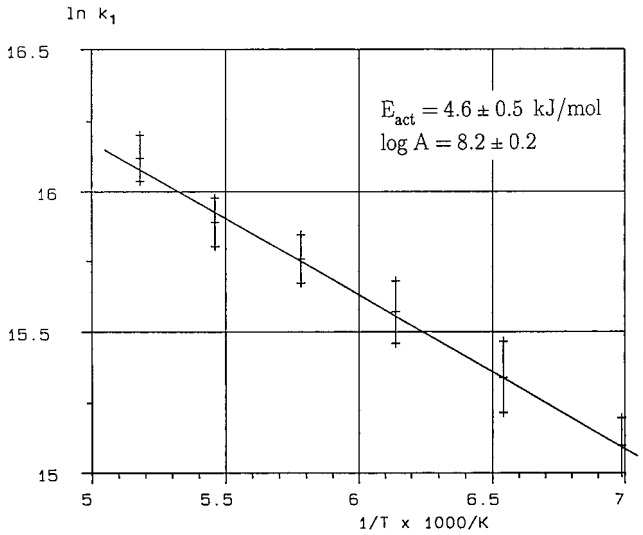

Figure 5. Arrhenius plot for the rate constant k_1 of the $CHCl_3^-$ fragmentation.

nm, the anion fragmentation is not observable, as both anions are not absorbing in this range. As seen at 600 nm (Figure 2b), the late linearity is valid up to $t^{-0.6} \approx 1.2\ \mu s^{-0.6}$ with a deviation downwards. This is the anchor point for the decay of the precursor M^{+}*, defining the rate constant $k_{tot} = k_{frag} + k_Q$. The same deviation is seen within the $CHCl_3^-$ absorption band (Figure 2a). As it overlaps with the anion fragmentation, the determination of k_{tot} is rather difficult in this λ range.

The First Step of Simulation. The simulation starts at the late end of geminate kinetics (small $t^{-0.6}$ values).[8] As we now know that the mobility value δ_2 is allowed to be λ dependent for mixed pairs, the linearity fitting becomes very satisfactory for the complete λ range. The experimental results for δ_2 are shown in Figure 3 for the temperatures 143, 153, and 173 K, and Figure 4 presents the corresponding intercept spectra ID_2. As the Cl^- anion is not absorbing in the complete λ range (from 350 to 750 nm), ID_2 represents the sum of the MCH^+ band (λ_{max} = 570 nm) and the $MCHene^+$ band (λ_{max} = 450 nm),[5] each with a fraction of the free ion yield, defined by the ratio of k_Q/k_{frag}. From Figure 4 it is obvious that this ratio increases with temperature, i.e., increased MCH^+ yield with reduced $MCHene^+$ yield and an overall G_{fi} increase.[4]

The Second Step of Simulation. The aim is to determine the anchor point for the anion fragmentation (the end point of the $CHCl_3^-$ decay[10]) and to search for δ_1 and ID_1. As the mobilities of Cl^- and $CHCl_3^-$ are expected to be very similar and small relative to the high mobility of MCH^+, it is expected that $\delta_1 \approx \delta_2$. For λ within the $CHCl_3^-$ band it is now possible to derive $k_1(CHCl_3^- \rightarrow Cl^-)$ (Table 1) and ID_1 with a few iterative cycles.

The fragmentation rate constants k_1 at 143, 153, and 173 K were derived by averaging the results for all λ within the $CHCl_3^-$ absorption band. The rate constants k_1 for other temperatures were determined at λ_{max} only (Table 1). An Arrhenius plot (Figure 5) yields E_{act} = 4.6 ± 0.5 kJ/mol and a very low pre-exponential factor of log A = 8.2 ± 0.2.

ID_1 differs from ID_2 by the $CHCl_3^-$ absorption (free ion yield). The details for the system at 153 K are shown in Figure 6. As the free ion yields are known (assumed linearity between G_{fi}(143 K) = 0.06 (100 eV^{-1}) and G_{fi}(293 K) = 0.12 (100 eV^{-1})[10]) the experimental spectrum $\epsilon_{CHCl_3^-}(\lambda)$ is determined quantitatively for the three temperatures 143, 153, and 173 K as shown in Figure 7. Simulation by a Lorentzian line shape[5] gives λ_{max} = 470 nm, ϵ_{max} = 1900 ± 30 M^{-1} cm^{-1} (statistical error only) and a half width at half maximum (hwhm) of 28 ± 2 nm.

The Final Step of Simulation. The last step of rate curve simulation covers $t^{-0.6} \gtrsim 1.2\ \mu s^{-0.6}$, the downward deviation. The lower limit corresponds to the anchor point for the M^{+}* decay, and $k_{tot} = k_{frag} + k_Q$ is derived from rate curves at $\lambda >$ 550 nm, where there is no interference from the $CHCl_3^-$ absorption. For a good value of k_{tot}, however, α and IA must also be known. We expect $\alpha(M^{+}*/CHCl_3^-)$ to correspond to $\beta(MCH^+/CHCl_3^-)$, the mobility of M^{+}* and MCH^+ assumed to be identical.[5] Eventually β will be derived from δ_1 for the primary mixed pair of ions ($MCHene^+$, $MCH^+/CHCl_3^-$) (see later). For the time being, $\beta(MCH^+/CHCl_3^-)$ is set equal to $\beta(MCH^+/N_2O^-)$ = 3.05 $\mu s^{0.6}$ at 143 K or 2.05 at 153 K[4] for

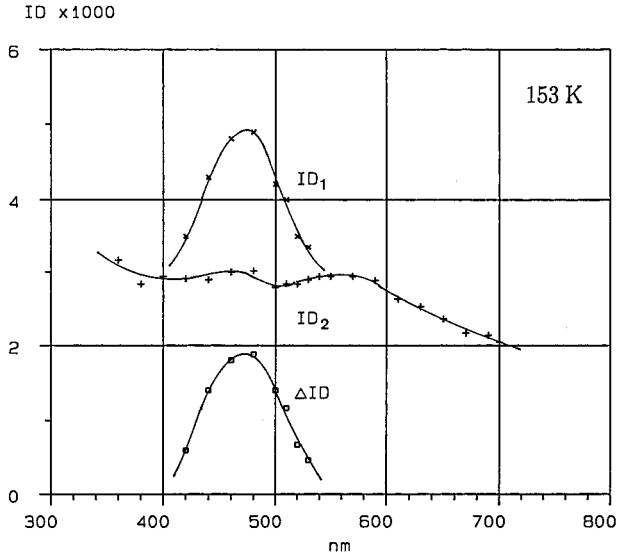

Figure 6. The free ion intercept spectra ID_1 ($MCHene^+ + MCH^+ + CHCl_3^-$) and ID_2 ($MCHene^+ + MCH^+$) from 0.2 M $CHCl_3$ in MCH at 153 K. The difference $\Delta ID = ID_1 - ID_2$ represents the free ion yield of $CHCl_3^-$.

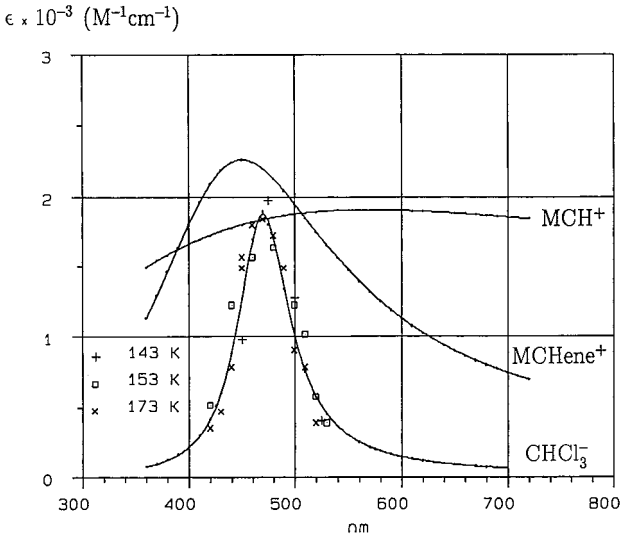

Figure 7. The absorption coefficients ϵ_i for MCH^+ and $MCHene^+$ [5] correspond to the Lorentzian lines with the following parameters: for $MCH^+ \rightarrow \lambda_{max} = 570$ nm, $\epsilon_{max} = 1910$ M^{-1} cm^{-1} and hwhm = 300 nm; for $MCHene^+ \rightarrow \lambda_{max} = 450$ nm, $\epsilon_{max} = 2260$ M^{-1} cm^{-1} and hwhm = 90 nm. For the chloroform anion, $CHCl_3^-$, the spectrum is derived from the ID differences at 143, 153, and 173 K (see example in Figure 6), using the known free ion yield G_{fi}.[4] The line represents the Lorentzian band fitted to the experimental points of all temperatures ($\lambda_{max} = 470$ nm, $\epsilon_{max} = 1900 \pm 30$ M^{-1} cm^{-1} and hwhm = 28 ± 2 nm). These spectra serve as the base for the simulation of $\delta(\lambda)$ with eqs 9−11.

N_2O-saturated MCH. This allows to simulate the earliest part of the experimental rate curve (for $t^{-0.6} > 1.3$ $\mu s^{-0.6}$ and $\lambda \geq 550$ nm); see Figure 2b.

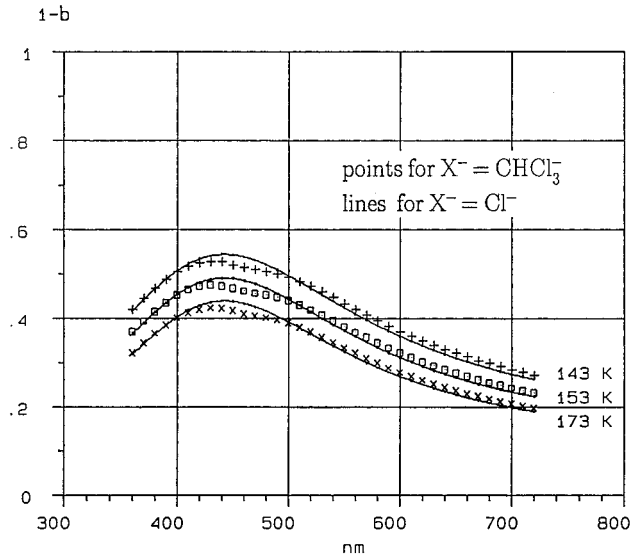

Figure 8. The fraction (1 − b) of eq 10 with which the slow mobility pair $\gamma(MCHene^+/X^-)$ is contributing to the mobility value δ of the mixed pairs of ions. For each of the temperatures 143, 153, and 173 K the factor (1 − b) was calculated for the two anions in the primary and secondary mixed pair: the points are used for $\epsilon^- = \epsilon(CHCl_3^-)$ and the lines for $\epsilon^- = \epsilon(Cl^-) = 0$.

The decay rate for $M^{+}*$ is $k_{tot}(143\ K) = (5.1 \pm 0.4) \times 10^6$ s^{-1} and $k_{tot}(153\ K) = (6.0 \pm 0.5) \times 10^6$ s^{-1} (Table 1). At 143 K the value k_{tot} ($CHCl_3$ as solute) may be compared with $k_{tot} = 6.1 \times 10^6$ s^{-1} (N_2O as solute).[5] This indicates that $CHCl_3$ must be less effective in quenching than N_2O.

The free ion intercept IA, available for $\lambda \geq 550$ nm, should represent $M^{+}*$ as $CHCl_3^-$ is not contributing in this λ range. The result is comparable with the known $M^{+}*$ spectrum,[5] though the absolute values are larger.

Simulation of $\delta(\lambda)$. From the experimental mobility values $\delta(\lambda)$ for the mixed pairs ($MCHene^+$, MCH^+/X^-) (Figure 3) and their theoretical prediction in eq 10, it is possible to derive the individual mobility values $\beta(MCH^+/X^-)$ and $\gamma(MCHene^+/X^-)$. The required absorption coefficients $\epsilon(MCHexene^+)$,[5] $\epsilon(MCH^+)$,[5] and $\epsilon(CHCl_3^-)$ are available and shown in Figure 7. Furthermore, $\epsilon(Cl^-) = 0$ for the present λ range. The ratio k_1'/k_1'' in eq 10 is now k_Q/k_{frag}. It may be derived from the experimental value $k_{tot}(= k_Q + k_{frag})$ and k_{frag} found in the system with N_2O-saturated MCH[5] (see Table 2). The latter is only known for 143 K. The value for 153 K was extrapolated from assumed temperature dependence. The resulting k_Q/k_{frag} ratios are 1.05 at 143 K and 1.2 at 153 K. For 173 K (no k_{tot} experimentally available), k_Q/k_{frag} is estimated to be ∼1.6 on the base of the experimental free ion yield ID_2 (Figure 4).

The factor b with which $\beta(MCH^+/X^-)$ is contributing to the δ value may now be calculated (see eq 10). Depending on $X^- = CHCl_3^-$ or $X^- = Cl^-$ (primary or secondary mixed pairs, δ_1 or δ_2) the factor b differs, because of the different ϵ^- values. Figure 8 displays the factor for (1 − b), the contribution of the slow pair, $\gamma(MCHene^+/X^-)$, for the two mixed pairs at the three

TABLE 2: Results Derived from the $M^{+}*$ Decay Rate (k_{tot})

temp K	solute	$k_{tot}/10^6$ s^{-1}	$k_{frag}/10^6$ s^{-1}	k_Q/k_{frag}	% yield $MCHexene^+$	% yield MCH^+	$k_0/10^6$ s^{-1}	$k_2/10^6$ M^{-1} s^{-1}
143	0.118 M N_2O[c]	6.1 ± 0.3	2.5 ± 0.5	1.70 ± 0.23	37 ± 3	63 ± 3	0.32 ± 0.16	30 ± 5
143	0.3 M $CHCl_3$	5.1 ± 0.4	2.5 ± 0.5[c]	1.05 ± 0.2	49 ± 5	51 ± 5	0.30 ± 0.15[c]	7.7 ± 2.6
153	0.2 M $CHCl_3$	6.0 ± 0.5	∼2.7[a]	1.22 ± 0.2	45 ± 5	55 ± 5	0.4 ± 0.2[a]	14.5 ± 3.0
173	0.2 M $CHCl_3$			∼1.6[b]	∼38	∼62		

[a] Extrapolated. [b] Estimated from ID_2 spectra (Figure 4). [c] Ref 5.

temperatures 143, 153, and 173 K. The contributions $(1 - b)$ with $CHCl_3^-$ or Cl^- for a single temperature differ very little. It is support for the earlier made assumption, that $\delta_1 \approx \delta_2$.

The two mobility values $\beta(MCH^+/X^-)$ and $\gamma(MCHene^+/X^-)$ are now the only parameters for curve fitting to $\delta(\lambda)$. The results are visualized in Figure 3 and the β and γ values at the three temperatures, 143, 153, and 173 K are given in Table 1. The β values turn out to be the same, within error limits, as in the N_2O-saturated MCH at the same temperature. This is support for our initial assumption for α (see above). At 173 K the β value is smaller than in the N_2O-saturated system. It is unlikely that MCH^+ moves faster in the presence of $CHCl_3$. The discrepancy is rather related to the fact that the data at 173 K are the least accurate.

Quenching of M^+*. From the rate data k_{tot}, k_{frag}, and k_0 (Table 2) it is possible to derive the quenching rate constant $k_2(M^+* + CHCl_3)$, also given in Table 2. At 143 K, quenching by $CHCl_3$ is about four times slower than quenching by N_2O.[5] The ratio of quenching to fragmentation (k_Q/k_{frag}) for M^+* is found to increase with temperature (Table 2). This suggests that fragmentation at room temperature might have much less importance, as it is strongly suppressed by the quenching with $CHCl_3$.

Lifetime. The lifetime of $CHCl_3^-$ with 280 ns is substantially larger than expected from gas phase data.[12] However, from a mechanistic point of view it was concluded a long time ago that $CHCl_3^-$ should live "long compared to the neutralization process".[13]

Comparison with Other Chlorocarbon Anions. Many chlorocarbons have anions with similar characteristics, as found for $CHCl_3^-$. In neat, liquid Freon-113 ($CFCl_2CF_2Cl$) at 239 K[14] the anion absorption peaks at $\lambda_{max} = 440$ nm with a band width of hwhm ≈ 60 nm. The anion lifetime was judged to be "longer than μs". This corresponds to the many long lived anions of fluorocompounds.[15] For dichloromethane (CH_2Cl_2),[16] chloromethane (CH_3Cl),[17] and tert-butylchloride (t-BuCl)[18] in MCH, the anion bands peak again in the range from 440 to 460 nm. The band widths, at first sight, appear wide as for $CHCl_3^-$ in Figure 1, yet after correction for the solvent cations (MCH^+ and $MCHene^+$) it is expected that they are also narrow. For CCl_4 Klassen et al.[19] reported about a CCl_4^- transient absorption ($\lambda_{max} = 370$ nm) in a 3-methylpentane glass at 75 to 123 K, with a small band width (hwhm ≈ 28 nm), very similar to the one derived for $CHCl_3^-$ (Figure 7). The absorption coefficient ($\epsilon(CCl)^-_{max4} = 1.1 \times 10^4\ M^{-1}\ cm^{-1}$), however, is nearly 60 times larger. The comparison of CCl_4^- with $CHCl_3^-$ is hampered by the fact that CCl_4^- only exists in solid matrixes (and clusters). The transition in CCl_4^- most likely is due to a strong caging effect in the matrix. It is not characteristic for the molecular anion. Contrary to this, $CHCl_3^-$ only suffers a weak solvent effect.

VI. Conclusion

It has been possible to simulate the complete reaction mechanism of the geminate ion processes in methylcyclohexane with chloroform as solute. It includes parallel decay reactions of the cation to produce mixed pairs of geminate ions with $MCHene^+$ and MCH^+ and a simultaneous fragmentation of the primary anion $CHCl_3^-$. The fragmentation rate of $CHCl_3^-$ is accessible, because it is slower than the M^+* decay, but still within the time range of the geminate ion recombination.

The results clearly confirm the fact that the initial cation M^+* suffers fragmentation and quenching in parallel, quenching being dependent on the solute and its concentration. Because of the occurence of mixed pairs of geminate ions, the solvent MCH suffers some kinetic complications. On the other hand it presently represents the best known solvent for geminate ion kinetics.

The $t^{-0.6}$ kinetic law clearly allows to describe this complicated ionic mechanism rather well. It remains a powerful tool to handle geminate ion kinetics.

Acknowledgment. Support by the Swiss National Science Foundation and by the Research Funds of the ETH Zürich is gratefully acknowledged.

References and Notes

(1) Katsumura, Y.; Bühler, R. E. *Radiat. Phys. Chem.* **1989**, *34*, 543.
(2) van den Ende, C. A. M.; Warman, J.; Hummel, A. *Radiat. Phys. Chem.* **1984**, *23*, 55.
(3) Bühler, R. E. *Can. J. Phys.* **1990**, *68*, 918.
(4) Katsumura, Y.; Azuma, T.; Quadir, M. A.; Domazou, A. S.; Buhler, R. E. *J. Phys. Chem.* **1995**, *99*, 12814.
(5) Bühler, R. E.; Katsumura, Y. *J. Phys. Chem.* **1998**, *102*, 111.
(6) Bartczak, W. M.; Hummel, A. *Radiat. Phys. Chem.* **1994**, *44*, 335.
(7) Bühler, R. E., *Proceedings of the Trombay Symposium on Radiation and Photochemistry TSRP 98*, BARC, Trombay, Mumbai, India, Jan. 14−19, **1998**, part II, p 429.
(8) Bühler, R. E. *Res. Chem. Intermed.* **1999**, *25*, 259. Due to fateful printing errors, ask the author for a reprint.
(9) Hurni, B.; Brühlmann, U.; Bühler, R. E. *Radiat. Phys. Chem.* **1975**, *7*, 499.
(10) "Anchor point" corresponds to the "end point" of an ion reaction. Because of the late time compression in a $t^{-0.6}$ plot the rather undefined end point of a reaction is sharpened up.[8]
(11) Allen, A. O. National Bureau of Standards report Nr. NSRDS-NBS 57, **1976** or Baxendale, J. H.; Bell, C.; Wardman, P. *J. Chem. Soc., Faraday Trans. I* **1973**, *69*, 776.
(12) Shimamori, H., **1997**, private communication.
(13) Bühler, R. E. In *Chemistry of the Carbon Halogen Bond*, Patai, S., Ed.; J. Wiley & Sons: New York, 1973; Part 2, p 855.
(14) Hurni, B.; Bühler, R. E. *Radiat. Phys. Chem.* **1980**, *15*, 231.
(15) Christophorou, L. G. *Atomic and Molecular Radiation Physics*; Wiley-Interscience: New York, 1971, p 501.
(16) Katsumura, Y.; Bühler, R. E., to be published. See also ref 1.
(17) Domazou, A. S.; Studer, M.; Bühler, R. E., unpublished.
(18) Gębicki, J. L., Bühler, R. E., to be published.
(19) Klassen, N. V.; Ross, C. K. *J. Phys. Chem.* **1987**, *91*, 3668. Klassen, N. V.; Ross, C. K. *Chem. Phys. Lett.* **1986**, *132*, 478.